

Heating Properties of Non-invasive Hyperthermia Treatment for Abdominal Deep Tumors by 3-D FEM

E.Morita, K.Kato, S.Ono, Y.Shindo, K.Tsuchiya, and M.Kubo

Abstract— This paper discusses the heating properties of a new type of hyperthermia system composed of a re-entrant type resonant cavity applicator for deep tumors of the abdominal region. In this method, a human body is placed in the gap of two inner electrodes and is non-invasively heated with electromagnetic fields stimulated in the cavity.

Here, we calculated temperature distributions of a simple human abdominal phantom model that we constructed to examine the heating properties of the developed hyperthermia system. First, the proposed heating method and a simple abdominal model to calculate the temperature distribution are presented. Second, the computer simulation results of temperature distribution by 3-D FEM are presented.

From these results, it was found that the proposed simple human abdominal phantom model composed of muscle, fat and lung was useful to test the heating properties of our heating method. Our heating method was also effective to non-invasively heat abdominal deep tumors.

I. INTRODUCTION

HYPERTHEMIA is a method of cancer treatment based on the clinical fact that cancer cells are more sensitive than normal tissue in the temperature range of 42-44 °C, and they can be killed by one hour repetitions of one hour heating. A variety of heating methods has been already proposed to heat deep tumors. Examples, RF capacitive heating applicators and microwave heating applicators. These methods have both advantages and disadvantages, but a superior technique has not been created yet.

Therefore, we propose a new heating method which uses the large size re-entrant type resonant cavity for heating deep tumors in the abdominal region of the human body. This heating system was developed for non-invasive hyperthermia treatment.

First, we present a simple phantom model of the human abdominal region. This method was designed to calculate the temperature distribution by 3-D FEM.

Second, numerical results of the heating method determined by computer simulations are presented.

From these results, it was shown that the proposed heating method is effective to heat deep abdominal tumors.

E. Morita, K. Kato, S. Ono, Y. Shindo and K. Tsuchiya are with the Department of Mechanical Engineering Informatics, Meiji University, Kawasaki, Japan

M. Kubo is with the Future Creation Laboratory, Olympus Co., Ltd., Japan.

E-mail: ce82054@isc.meiji.ac.jp

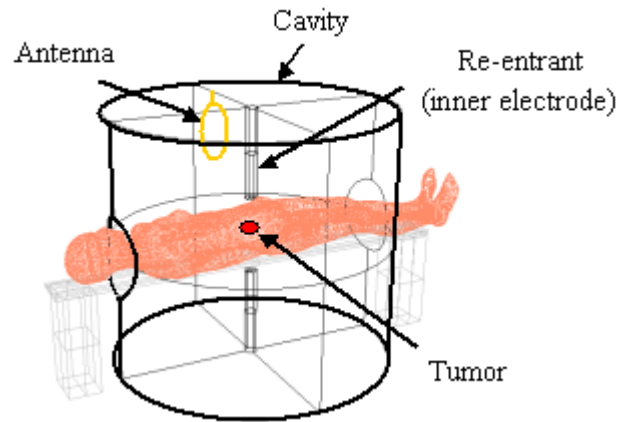


Fig. 1. Illustration of heating system.

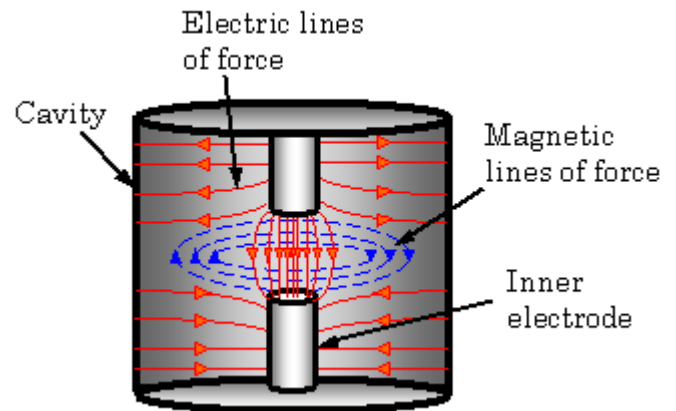


Fig. 2. Electric and magnetic field patterns.

II. METHODS

Fig. 1 shows an illustration of our heating system [1], [2]. In Fig. 1, a human body is placed between inner electrodes and is non-invasively heated without contact between the body surfaces and the applicator by the electromagnetic fields inside the cavity. Electric and magnetic field patterns for the TM_{010} -like mode of the cavity are shown in Fig. 2 [3]. This mode is the lowest of all the frequencies for heating deep tumors.

The tissue temperature (T) in a human body heated by the electromagnetic energy can be calculated by equations (1)-(5):

$$\rho c \frac{\partial T}{\partial t} = \text{div}(\kappa \cdot \text{grad}T) + W_h - W_c + M \quad (1)$$

$$W_h = \frac{1}{2} \sigma |E|^2 \quad (2)$$

$$\nabla^2 E + k^2 E = 0 \quad (3)$$

Boundary condition at the cavity wall,
 $n \times E = 0$

$$W_c = (F\rho)_{\text{tissue}} \times (\rho c)_{\text{blood}} \times (T - T_b) \quad (4)$$

$$M = M_0 (1.1)^{\Delta T} \quad (5)$$

Where ρ is the volume density of tissue, c is the specific heat of tissue, κ is the thermal conductivity, σ is the electrical conductivity, $k^2 = \omega^2 \epsilon \mu$, ω is the radial frequency, ϵ is the dielectric constant, μ is the magnetic permeability, F is the blood flow rate, T_b is the blood temperature, M_0 is the basal metabolic heat. Equations (1) and (3) can be solved numerically by using the finite element method (FEM). In this study, we assume that both W_c and M in the equation (1) can be neglected, because an agar phantom is used in computer simulations.

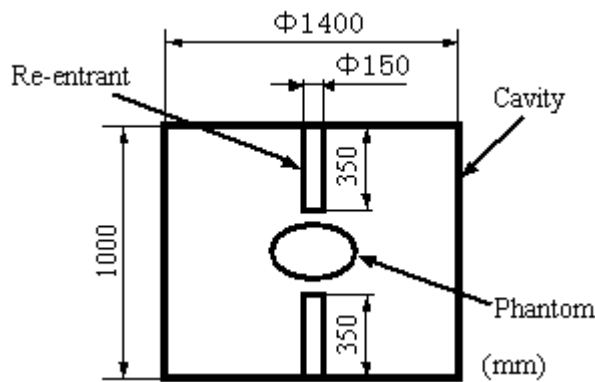


Fig. 3. Re-entrant resonant cavity.

TABLE I
PHYSICAL PARAMETER VALUES OF PHANTOM

	ϵ_r	σ (S/m)	ρ (Kg/m ³)	κ (W/m ² °C)	c (J/Kg°C)
Phantom	80	0.6	1000	0.6	4200
Air	1	0	1.165	0.025	1010
Lung	1	0	1.165	0.025	1010
Fat	13	0.009	900	0.22	2300

ϵ_r = Relative dielectric constant, σ = Electrical conductivity,
 κ = Thermal conductivity, ρ = Volume density, c = Specific heat.

III. ANALYTICAL MODEL

Fig. 3 shows the diagram of the dimensions determined by computer simulations. Similar to human dimensions, the cavity was 1,400 mm in diameter and 1,000 mm in height. To concentrate the heating energy in the center of the cavity, the inner electrodes were 50 mm in diameter and 350 mm in height.

Fig. 4 shows a simple human phantom model based on the human abdominal region. This phantom is elliptic in shape and consists of muscle, fat and lung. The fat layer is 20mm thick.

The physical parameter values of the phantom used in the FEM calculation are listed in Table I.

Fig. 5 shows a finite element mesh for calculating the electromagnetic field and temperature distributions. The boundaries were set to the room temperature 30 °C. Initial conditions were set to body temperature 37 °C. Here JMAG-studio (JSOL Co.Ltd, Japan) was used in computer simulations.

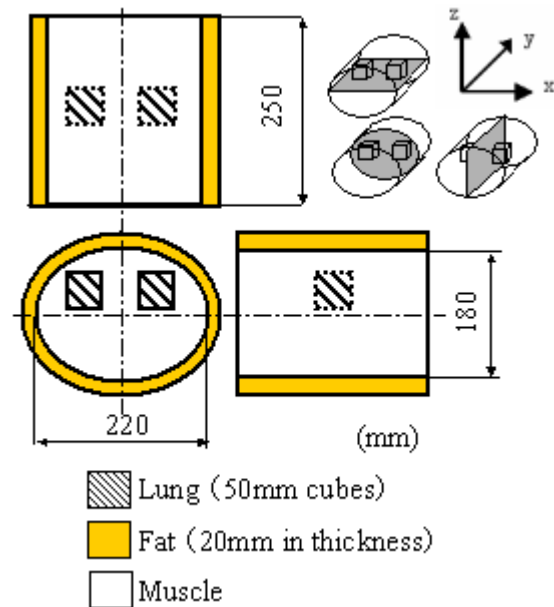


Fig. 4. Illustration of phantom model.

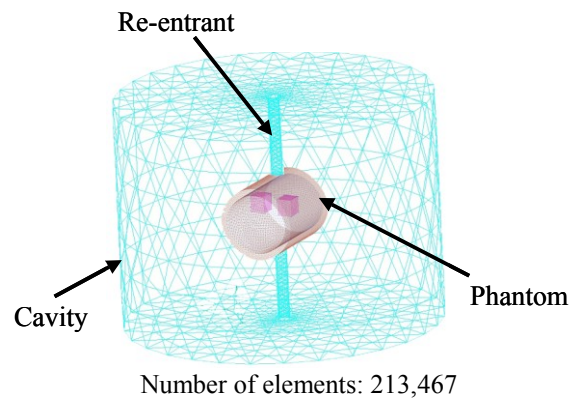


Fig. 5. Finite element mesh for calculating electromagnetic field and temperature distributions.

IV. RESULTS AND DISCUSSION

A. Muscle equivalent phantom

Fig. 6 shows the results of temperature distributions of slices of the elliptic cylinder type muscle equivalent phantom estimated by the computer simulation. In Fig. 6, cross-sections (b), (d) and (f) respectively correspond with temperature diagrams (a), (c) and (e). Heating time was 30 minutes. In Fig. 6, it has been found that the center region of the phantom was heated to a maximum temperature of 42-43°C. Fig. 7 shows the thermal image of the sagittal slice of the phantom taken by an infrared thermal camera after 40 minutes of heating. Fig. 8 shows the measured and estimated temperature profiles along the x and z-axes. The measured temperature agrees with the estimated temperature with an error of 15% or less at the normalized temperature 0.8. The normalized temperature T_N is given by equation (6)

$$T_N = \frac{(T - T_0)}{(T_{\max} - T_0)} \quad (6)$$

Where T_0 is the initial temperature, T_{\max} is the maximum temperature inside the phantom. Therefore, it was confirmed that computer simulation by using FEM is useful to estimate the temperature distribution.

B. Muscle- lung phantom

Fig. 9 shows the estimated computer simulation results of temperature distributions of a slice of the muscle-fat phantom. From Fig. 9, it was found that a hot spot appeared at the center region of the phantom as seen in the case of the heating of the muscle equivalent phantom heating. However, in Fig. 9(a), hot spots are found in the fat layer. The generation of this hot spot was due to the fact that the muscle and fat layers were arranged in tandem for current flows and as electrical field intensity increases. Therefore, exothermic energy increases in the vicinity of the fat layer. It is probable that cooling the surrounding fat layer can control the generation of the hot spot.

C. Muscle- lung-fat phantom

Fig. 10 shows the results of temperature distributions in the slice of the muscle-lung-fat phantom estimated by the computer simulation. In the present calculated conditions, for simplicity, physical parameter values of the lung used in the FEM were assumed to be that of air. Parameter values of an in-vivo lung are difficult to determine, because live subject is always breathing. As shown in Fig. 10, a hot spot was created in the space between the lungs. The generation of the hot spot was due to the fact that the electric conductivity of the lung is assumed to be zero and current flows through the space between the lungs.

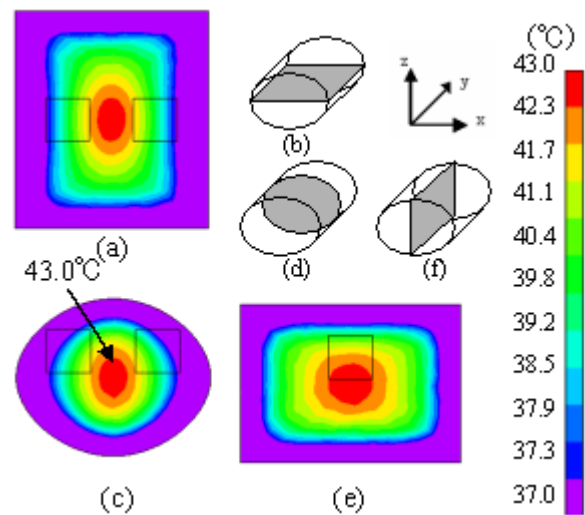


Fig. 6. Estimated temperature distributions of elliptic cylinder type muscle equivalent phantom after 30 minutes of heating.

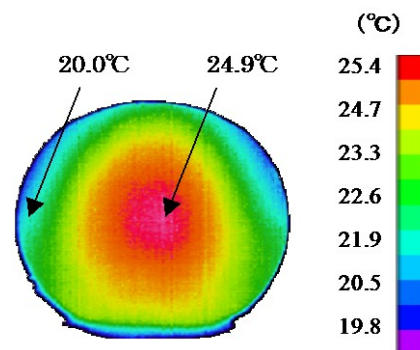


Fig. 7. Thermal image of agar phantom.

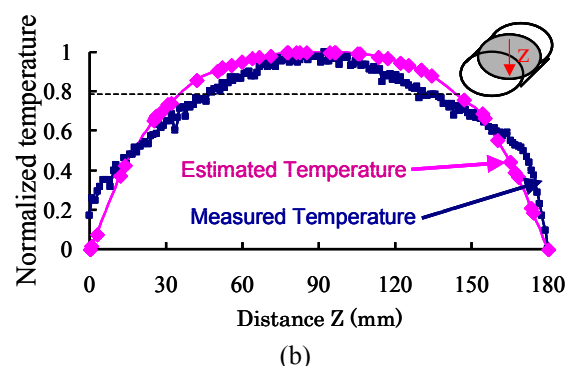
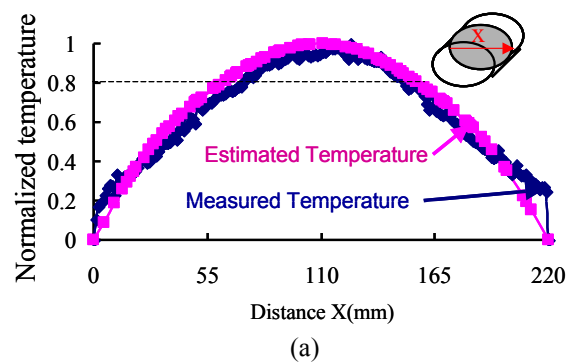


Fig. 8. Temperature profiles

ACKNOWLEDGMENT

This work was supported in part by Grants in Aid for Scientific Research (C) (20591484) from the Ministry Education, Culture, Sports, Science, and Technology of Japan.

REFERENCES

- [1] R.F Tumor, "Regional hyperthermia with an annular phased array" *IEEE trans. Biomed. Eng.*, vol.31, no.1, pp.106-114, 1984.
- [2] J. J. W.Langendijk, "A new coaxial TEM radiofrequency/ microwave applicator for non-invasive deep-body hyperthermia", *J. microwave Power.*, vol.18, pp.367-375,1983
- [3] J. Matuda, K. Kato and Y. Saitoh, "The application of a re-entrant type resonant cavity applicator to deep and concentrated hyperthermia", *Jpn. J. Hyperthermia Oncol.*, vol. 4 no. 2,pp.111-118,1988

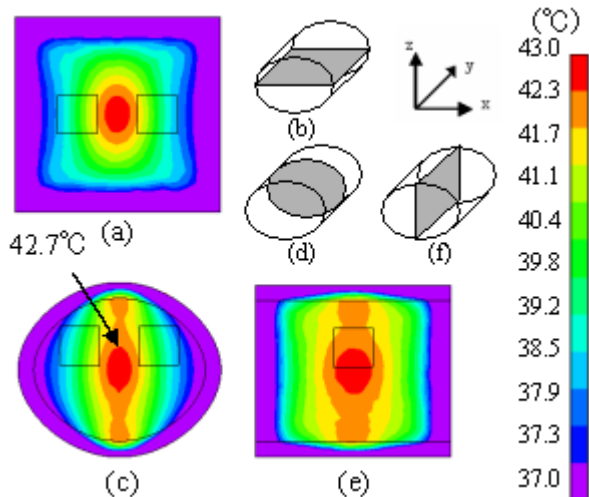


Fig. 9. Estimated temperature distributions of muscle-fat phantom after 30 minutes of heating.

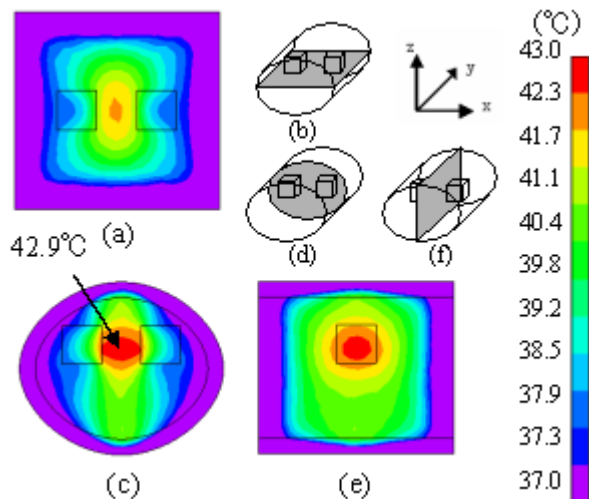


Fig. 10. Estimated temperature distributions of muscle-fat-lung phantom after 30 minutes of heating.

V. CONCLUSION

In this paper, we proposed a new heating method which uses the large size re-entrant type resonant cavity for heating deep tumors in the abdominal region of the human body.

It was found that the proposed simple human abdominal phantom model composed of muscle, fat and lung was useful to simulate the heating properties of our heating method and our heating method was also effective to non-invasively heat deep abdominal tumors.

In this study, we had used an elliptic cylinder type model for a basic analysis. However, the human body is a complex structure. Therefore, we are now studying to confirm the possibility of experimental clinical heating for various types of deep-seated tumors using the human anatomical model.